Oil & Natural Gas Technology

DOE Award No.: DE-FE0000408

Quarterly Report

October 2010 – December 2010

Post Retort, Pre Hydro-treat Upgrading of Shale Oil

Submitted by:
Ceramatec Inc
2425 S. 900 W.
Salt Lake City, UT 84119

Prepared by: John H. Gordon, PI

Prepared for:
United States Department of Energy
National Energy Technology Laboratory

January 28, 2010

Office of Fossil Energy

TABLE OF CONTENTS

LIST OF FIGURES

LIST OF TABLES

LIST OF APPENDICES

None

EXECUTIVE SUMMARY

In the 5th quarter considerable progress was made with regard to the reactor side and electrolysis side of the upgrading process. Sodium is becoming the frontrunner. Sulfur and nitrogen removal is best when sodium is utilized for all three oil stocks tested while the electrolysis of sodium sulfide is looking better than electrolysis of lithium. In the 5th quarter the electrolysis was performed for the first time at a temperature above the melting point of sodium. Current density increased two orders of magnitude while degradation of the membrane became negligible. Upgrading with methane as the hydrogen donating gas also is showing promise.

Expenditures to date are close to budget.

PROGRESS, RESULTS, DISCUSSION

Task 1.0: Project Management Plan

The PMP was updated within 30 days and submitted to the Project Manager (Quarter 1).

Task 2.0: Upgrading Development

This task is related to developing the process of treating shale oil, or heavy oil at elevated temperature and pressure in the presence of an alkali metal, either sodium or lithium and also a hydrogen source, either hydrogen gas or methane (natural gas) to form an oil stream with reduced levels of sulfur, nitrogen and heavy metals and also in the process reducing the viscosity and increasing the API gravity. The object here is to determine the impact of various reaction parameters on product quality.

Sub task 2.1: Analytical Capability

Analytical Laboratory Set up

The Perkin-Elmer 2400 CHNS analyzer, due to several disadvantages that the manufacturer was not aware of, was returned. New CHNS from LECO will be arriving second week of February 2011. Meanwhile we continue to send the samples for analysis to Huffman Laboratories as well as LECO's in-house applications laboratory. The swap of instruments has not affected the progress of the project.

Sub-task 2.2: Upgrading Reactor and Separation Setup

Experimental

Several additional experiments were performed on upgrading of Red Leaf shale oil (RL), (oil shale Exploration Company shale oil (OSEC) and San Joaquin heavy crude oil (SJ) aimed towards parametric optimization. All the experiments were performed with using Sodium or Lithium as the alkali metal, 180 gm (approx.) of oil as raw material, 1000 psig pressure (approx) and H2 or CH4 as hydrogen donating gas. Upon reaction, the product was subjected to centrifuging to separate the solid fraction (sulfides and possibly heavy metals) from liquid. Table 1 below shows the list of different experiments.

Table 1: List of Experiments Performed

Expt #	Feed	Alkali metal	Upgrading gas	Quantity (g)	Time (hr)
1	RL	Na	H2	6.11	1
2	RL	Na	CH4	6.05	1
3	RL	Na	H2	13.62	2
4	RL	Li	H2	0.91	1
5	RL	Li	CH4	1.78	1
6	RL	Li	H2	4.19	2
7	OSEC	Na	H2	5.95	1
8	OSEC	Na	CH4	6.06	1
9	OSEC	Na	H2	6.33	2
10	OSEC	Na	H2	6.28	2
11	OSEC	Li	CH4	1.84	1

12	OSEC	Li	H2	1.89	2
13	SJ	Na	H2	5.95	1
14	SJ	Na	CH4	5.98	1
15	SJ	Na	H2	10.66	2
16	SJ	Na	CH4	10.66	2
17	SJ	Na	Ch4	10.66	2
18	SJ	Li	H2	1.84	1
19	SJ	Li	CH4	1.85	1
20	SJ	Li	H2	1.94	2
21	SJ	Li	H2	3.26	2
22	SJ	Li	CH4	3.2	2

Results and Discussions

1. CHNS

CHNS measurements were performed on raw material samples and product samples. Compositional analysis for all the three raw material samples is shown in Table 2 below and Table 3 lists analysis results for products.

Table 2: C, H, N and S Composition of Raw Materials

Raw material	C (%)	H (%)	N (%)	S (%)
RL	85.48	12.33	1.48	0.25
OSEC	84.83	12.74	0.47	0.84
SJ	85.70	11.27	0.76	1.54

Table 3: C, H, N and S Composition of Products

Experiment number	**C (%)**	**H (%)**	**N (%)**	**S (%)**
1 (RL)	85.86	13.05	0.64	0.03
2 (RL)	85.72	12.51	0.71	0.06
4 (RL)	85.71	12.28	1.35	0.22
5 (RL)	85.59	12.4	1.29	0.17
7 (OSEC)	86.41	13.36	0.16	0.02
8 (OSEC)	85.95	13.06	0.25	0.03
9 (OSEC)	86.37	13.53	0.18	0.03
10 (OSEC)	86.34	13.16	0.24	0.12
11 (OSEC)	86.04	12.92	0.33	0.37
12 (OSEC)	86.06	13.08	0.37	0.39
13 (SJ)	85.56	11.72	0.68	0.27
14 (SJ)	83.79	11.25	0.67	1.07
15 (SJ)	86.18	12.5	0.19	0.04
18 (SJ)	85.33	11.6	0.7	1.5
19 (SJ)	84.99	11.39	0.7	1.28
20 (SJ)	84.75	11.63	0.69	1.29
21 (SJ)	84.34	11.51	0.67	1.21

Table 4 shows the reduction in the ratio of nitrogen to carbon and sulfur to carbon by run. From the table we can see the best results have occurred with sodium as the alkali metal and where hydrogen was the donating gas. This was true for all three oil sources. In addition, in the case of the shale oil sample, using methane also showed encouraging results when sodium was the alkali metal.

Table 4: Nitrogen and sulfur reduction by run

Run	Oil	Gas	Alkali	N reduction	S reduction	Act Alk/Theo	Hours
1	RL	H2	Na	57%	88%	0.45	1
2	RL	CH4	Na	52%	76%	0.43	1
4	RL	H2	Li	9%	12%	0.22	1
5	RL	H2	Li	13%	32%	0.43	1
7	OSEC	H2	Na	67%	98%	0.94	1
8	OSEC	CH4	Na	48%	96%	0.94	1
9	OSEC	H2	Na	62%	96%	0.98	2
10	OSEC	H2	Na	50%	86%	0.98	2
11	OSEC	CH4	Li	31%	57%	0.98	1
12	OSEC	H2	Li	22%	54%	0.98	2
13	SJ	H2	Na	10%	82%	0.58	1
14	SJ	CH4	Na	10%	29%	0.56	1
15	SJ	H2	Na	75%	97%	0.99	2
18	SJ	H2	Li	7%	2%	0.58	1
19	SJ	CH4	Li	7%	16%	0.58	1
20	SJ	H2	Li	8%	15%	0.60	2
21	SJ	H2	Li	10%	20%	1.01	2

2. Inductive Coupled Plasma (ICP)

Inductive coupled plasma measurements were performed for all three feedstocks and output of two experiments of SJ, expt 15 and 21. Table 5 below shows the results of ICP measurements on feedstocks and Table 6 below shows the measurements from expt 15 and 21.

Table 5: ICP measurements on different feedstocks

Element/Feed	Fe	Al	Cr	Cu	Mo	Si	V	Zn	Ni	Hg	As	Co
RL	36.54	9.533	0	0.181	0	2.544	0.293	8.199	0.756	0	29.01	0
OSEC	0[1]	9.99	0	0	0	104	0.353	0.541	0	0	0	0
SJ	218	55.35	0	0	0	3.476	197	9.47	331.4	0	0	0

Table 6: ICP measurement of products

Expt	Fe	Al	Cr	Cu	Mo	Si	V	Zn	Ni	Hg	As	Co
15	0.781	8.171	0.468	2.19	0	2.266	0	12.15	0	0	0	1.654
21	0.071	5.557	0.411	0.023	0	0.502	0	2.834	0	0	0	0

---

[1] 0 is undetectable.

Conclusion

Results of sulfur and nitrogen removal are more promising with Na as the alkali metal compared to Li, in presence of hydrogen. When Na was used, up to 97.4% of sulfur was removed (SJ) and up to 75.1% of nitrogen (SJ) was removed. Similarly, up to 96.5% of sulfur was removed (Na, OSEC) and 52.5% nitrogen was removed in presence of CH4 as the hydrogen donating gas. ICP results from experiment 15 and 21 which were both from a heavy crude experiment indicate complete removal of vanadium and Nickel and near complete removal of iron. All the three metals removal plays a critical role in upgrading of the oil since refinery feedstock quality is stated in terms of Ni, V and Fe concentration.

Schedule

The progress of Task 2 is as per schedule.

Task 3.0 – Electrolysis Development

To reduce the overall cost of the upgrading process, an electrolysis process will be developed to regenerate sodium or lithium from the respective polysulfide. The process will feature ceramic ion conductive membranes developed at Ceramatec. The energy cost to regenerate the alkali metals from the polysulfide is expected to be about half that of producing the metals from their respective chlorides.

Subtask 3.1 – Membrane fabrication

The Recipient shall fabricate and characterize sodium conductive and lithium conductive membranes.

Comparison of Mechanical Strength of LiSICON 10B, with Secondary Phase, and Phase Pure LiSICON 10B

The Ring-on-Ring Test, per ASTM Standard C1499-04, was followed to obtain mechanical strength and weibull distribution data. The procedure was the same as the previous Ring-on-Ring Test conducted last quarter. The tests compared the new phase pure 10B, made from more pure raw materials, with the later 10B material that contained a small secondary phase of $LiTiPO_4$.

A total of 17 LiSICON 10B discs, with a secondary phase, were tested. Each of them had a thickness of 500µm and a diameter of 24mm. A Weibull plot was used to represent the distribution of the strength data and to determine the Weibull modulus of the material (Figure 1). The material had a characteristic strength of 52.8MPa and a Weibull modulus of 4.9.

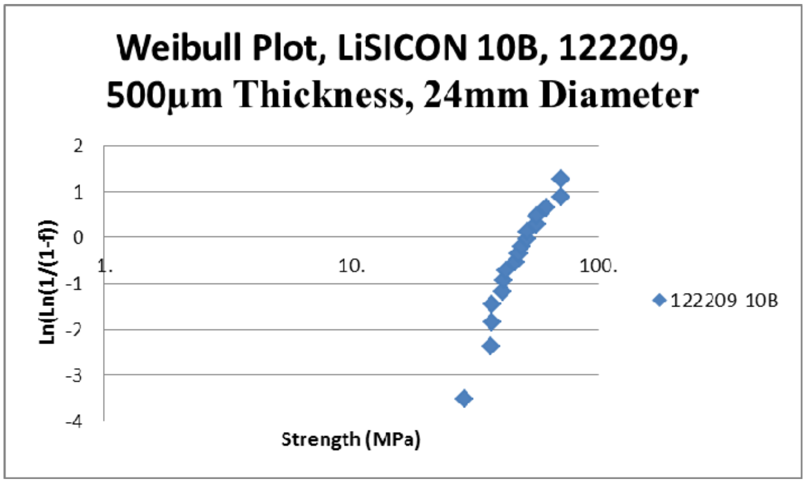

Figure 1. Weibull plot of LiSICON 10B with secondary phase.

A total of 17 phase pure LiSICON 10B disks were tested.The dimensions of the discs were 500µm thick and 24mm in diameter. From the Weibull plot below, Figure 2, the characteristic strength is 130 MPa and the Weibull modulus is 8.3.

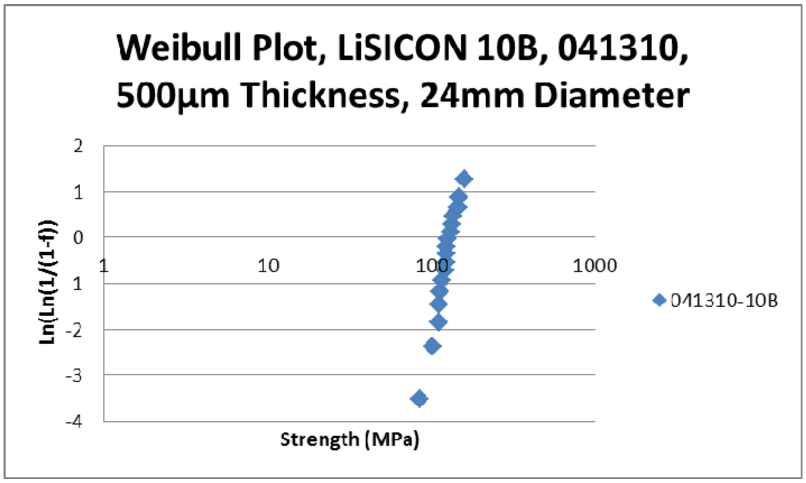

Figure 2. Weibull plot of phase pure LiSICON 10B.

The results show that the LiSICON 10B phase pure material is 2.5 times stronger than the material with the secondary phase. In addition, there was also a significant increase in the Weibull modulus from 4.9 to 8.3. This means that the population of phase pure LiSICON 10B samples tested has a much tighter distribution of strengths than the secondary phase population.

Subtask 3.2 – Seal testing

Ceramatec shall evaluate various seal approaches for compatibility with the alkali metal and the metal polysulfide at various temperatures.

We have completed the evaluation of four different high temperature epoxy formulations for sealing NaSICON disks to alumina tubes in the molten sodium recovery test cells. Out of the four products tested, only two have demonstrated some success in the presence of molten sodium and the anolyte solution (sodium polysulfide in MF) up to temperature of 120°C. In general, the maximum seal life time at those temperatures is approximately 30 to 40 hours. During the next reporting period, a glass seal material, that has a close CTE match between NaSICON and alumina, will be tested as an alternative to the epoxies.

Subtask 3.3 – Cell design and set up

Ceramatec shall design benchtop cells for two types of operation, one where the alkali metal is molten and one where it plates onto a current collector. Reactors and catholyte transfer means will be provided to prepare alkali metal sulfide of differing composition and transfer to the cell. The cells will be designed to accommodate multiple reference electrodes, operate at various elevated temperatures. The cells will have features designed to facilitate sulfur removal and be designed to operate within a dry enclosure.

Electrolysis Test Cell Design

Molten sodium recovery test cells have been built and tested for the first time during this period. The experimental setup (Figure 3) consisted of a glass flask containing the anolyte (~250 to 400 ml) and a 1” in diameter alumina tube with a 1” in diameter NaSICON-GY membrane epoxied to one end of the tube. A small amount of sodium metal (~1 to 3 grams) is pressed to size and introduced inside the tube against the NaSICON membrane. Then, the tube is submerged inside the anolyte solution, where the sodium is slowly heated up until it melts. A titanium rod is used as a current collector between the molten sodium catholyte and the external electrical circuit. The anolyte solution is agitated during the test and the temperature of the cell is maintained constant. The cell was run within the temperature range 110-130ºC. For safety reasons, pure TG was first used as anolyte solvent to avoid the reaction with sodium metal in case of a seal failure. However, the low ionic conductivity and low polysulfide solubility of the solvent allowed the cell to run only at very small current densities. The reactivity of mixtures of TG and MF solvents with sodium metal were evaluated. It was finally decided to use pure MF and to run all the experiments under a nitrogen blanket inside the glove box.

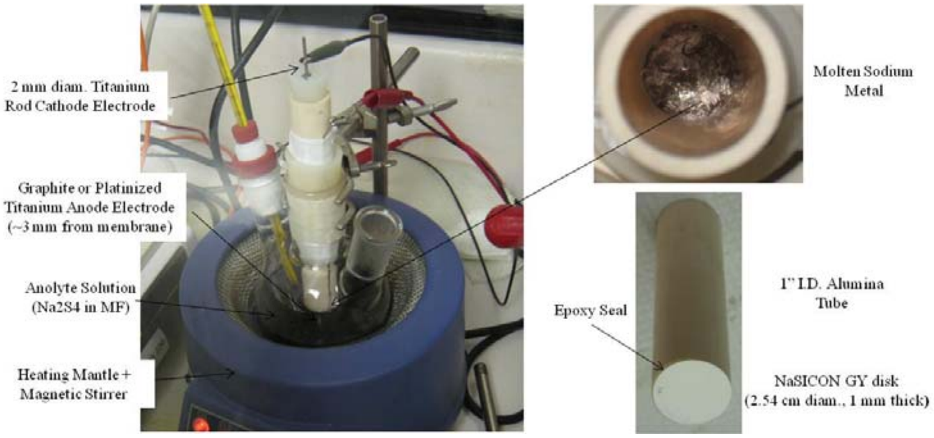

Figure 3. Molten sodium recovery test cell setup

Six recovery cells of the new design (Dual Flow Test Cells) have been fabricated and assembled. The cells have proven to be hermetic at 30 psig and ambient temperature using water as test fluid. These cells will be used to generate data of the alkali metal recovery process at low temperature (below molten). In addition, a lab experimental setup to run the catholyte and anolyte solutions, on a continuous closed-loop arrangement, through the cell has been built (Figure 4). The setup has the capability to heat-up and maintain the electrolyte solutions up to the cell desired operating temperature. The initial runs will be all conducted at ambient temperature conditions.

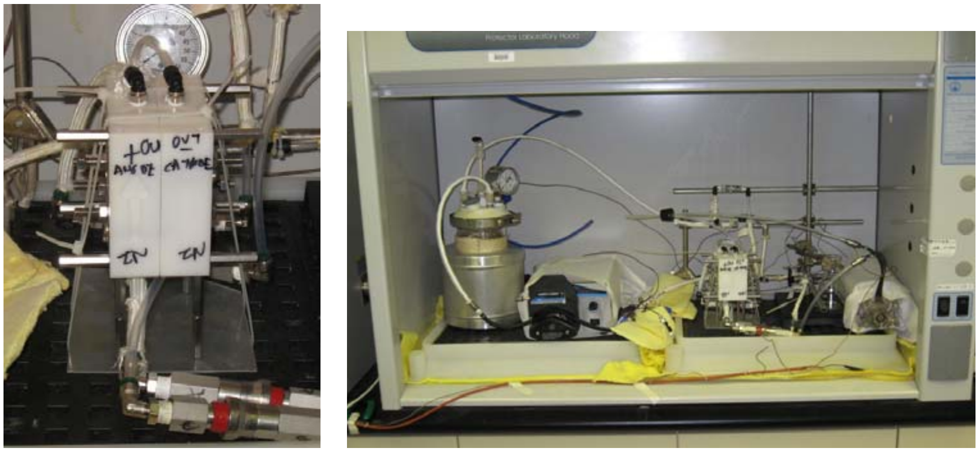

Figure 4. Dual Flow Recovery Test Cell [A] and lab experimental setup for the closed-loop continuous process [B]

<u>Subtask 3.4 – Cell operation</u>

The Recipient shall operate cells under various conditions including variation of the current density, electrode gap, temperature, electrolyte, polysulfide order, and alkali metal. Current will *be measured as a function of applied voltage. Periodically cell operation will be interrupted and cell contents analyzed to determine current efficiency. In Phase 1 the alkali metal polysulfide will be synthesized from alkali metal and sulfur and will not contain appreciable impurities which may flow through from an actual upgrading process as will occur in Phase 2.*

Effect of Temperature on the Ionic Conductivity of the Anolyte

The ionic conductivity of the anolyte solution (Na_2S_4+MF), used in the sodium recovery cells, has been measured within the temperature range 21-100°C. Higher temperatures could not be covered due to the limitation of the instrument used. Figure 5 shows the ionic conductivity versus temperature for electrolyte solutions containing 0.25M and 0.5M sodium polysulfide. The data shows excellent linearity within the temperature range covered. The ionic conductivity approximately doubled going from ambient temperature to 100°C. The high ionic conductivity of the solution assures that the contribution of the anolyte to the overall cell resistance in molten sodium recovery cells is small.

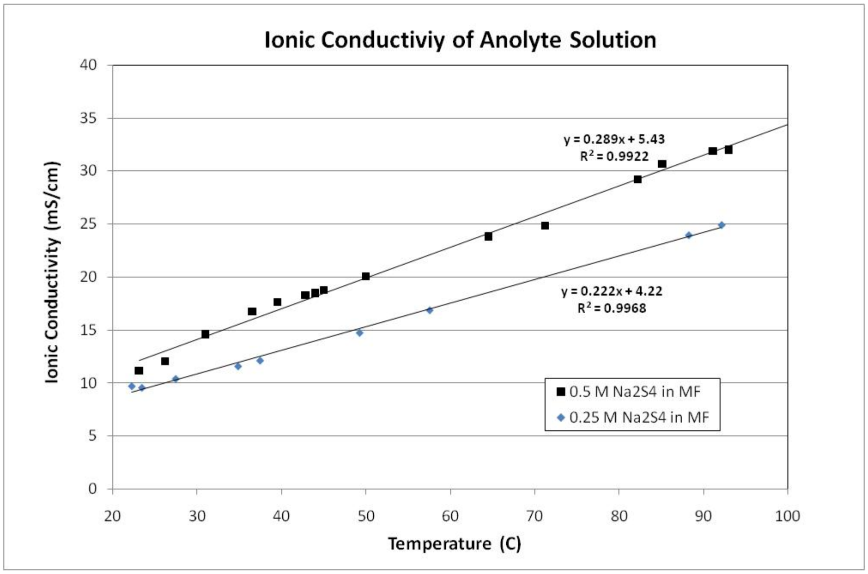

Figure 5. Ionic conductivity vs. temperature of the anolyte solution in sodium recovery cells

Test Cell Runs Results

Molten Sodium Recovery Test Cell Runs

A total of 12 molten sodium recovery test cells have been assembled and run during this reporting period. Table 7 summarizes the test cells construction properties and the runs operating conditions. The main focus of the initial runs was to evaluate the proper ratio of TG and MF in the anolyte solution. As mentioned earlier, it was decided to use pure MF to maximize the ionic conductivity of the solution and the polysulfide solubility. In addition, the cell was operated under a dry nitrogen atmosphere to eliminate the fire hazards associated with the potential failure of the anode-cathode seal. The effects of different initial Na_2S_4 concentrations (0.02M to 0.5M) and the operating temperature (110-120ºC) on the cell's performance were analyzed. The cells were run in constant current mode during the first two tests. Constant voltage mode (5 to 6 V), however, was used for the remaining runs. In constant voltage mode, the current is not fixed and it can change according to the cell's resistance. In this way, the current density through the cell is always the maximum possible at the given constant voltage. Most of the NaSICON GY disks used in the cells were 1 mm thick. Titanium and Platinized Titanium mesh were used as electrodes on the anode side of the cell. Two different high temperature epoxy formulations (Duralco 4461 and Aremco 631) were used as anode-cathode seal materials. These two materials were selected from a group of five epoxies, which were previously tested. The main conclusions learned from these runs are summarized below.

1. Cyclic Voltammetry data (voltage sweeps) show the sodium ion to sodium metal reduction reaction to be extremely selective and reversible within the 2 to 6 volts range covered (Figure 6). The current vs. voltage curves obtained from successive voltage sweeps overlap each other, which demonstrates that no cell polarization or other deactivation process occurs during the measurements.
2. Very high maximum current densities (up 130 mA/cm^2 with cell *Na_molten_20101208* at 5 VDC) have been demonstrated with the last set of runs. This value is approximately two orders of magnitude higher than the highest achieved with the previous low temperature (below molten) sodium recovery cells tested in this research work. The data show that at these high current densities, the cell becomes mass transfer limited. This can be observed in Figure 6, where the current vs. voltage curve starts to deviate from a straight line at 4.2 V for the cell *Na_molten_20101116*. Therefore, increasing the cell operating temperature, increasing the sodium polysulfide concentration, and/or increasing the agitation in the anolyte solution all help to be able operate the cells at even higher current densities.

Formatted: Bullets and Numbering

3. Under no polarization or mass transfer limitation conditions, the overall cell resistance is determined by the sum of the ohmic resistance contributions of the NaSICON membrane and the anolyte solution. Therefore, the higher the ionic conductivity of these two components the lower the cell's overall resistance. In the cells with mixtures of TG and MF, as anolyte solvent, the anolyte was the dominant resistance. However, in the test cells with 100% MF and much higher Na_2S_4 concentrations, the NaSICON membrane became the main contributor to the overall cell resistance. This is illustrated in Figure 7, which shows the theoretically predicted anolyte solution and NaSICON membrane (1 mm thick) ohmic resistances versus the cell operating temperature. The figure also plots the maximum predicted cell current density vs. temperature, assuming no polarization or mass transfer limitations. The ohmic resistance data, measured in the test cell runs, compares reasonably well with the theoretically predicted values.
4. Figures 8 and 9 show the current density and the total anolyte sodium recovery (%) versus elapsed time for test cell runs *Na_molten_20101129* and *Na_molten_20101208*, respectively.

The results of these two runs are representative of most of the data collected in this set of runs. The peak (peak C.D) and the average (Avg. C.D) current densities are included in the figures. After an initial adjustment period, the cell current density decreases linearly with time as the sodium ions in the anolyte solution get depleted. This is the typical behavior of a batch, mass transfer controlled electrolytic reaction. The overall reaction rate becomes proportional to the bulk sodium and polysulfide ions concentrations in the anolyte solution. The proportionality constant is the mass transfer coefficient, which is mostly a function of cell temperature, anolyte agitation rate, and cell geometry. Figure 8 shows the importance of agitation in the reaction rate as demonstrated by the drop in current density when agitation was momentarily lost. As the reaction is taken to completion, the current density will eventually drop to zero. We have achieved a total sodium recovery over 90% in two of the runs. Actually, we could have reached that recovery level in every run had the seals not failed. In the run with cell *Na_molten_20101129* (Figure 9), extra sodium polysulfide was added to the cell after 26 hours of operation. The effect was an increase in the cell's current density in response to the increase of the reaction driving force (higher sodium and polysulfide ion concentrations). Another effect that should be noted is the decrease of the ionic conductivity of the anolyte solution as the total ions concentration decrease through the course of the reaction.

5. The reliability of the NaSICON GY planar membranes (1 mm thick) has proven to be quite impressive with no cracking, staining or dendrite formation after 30+ hours of testing at high current densities. In fact, all the runs were ended not because of membrane failure, but because of the loss of hermiticity or breakdown of the epoxy cathode to anode seal. This excellent reliability contrasts with the poor results found, a few months ago, when the same ceramic material was used in the low temperature (below molten) sodium recovery cells. Our hypothesis is that the high failure rate in that case was related to the presence of sodium metal particles in contact with the membrane during cell operation.
6. As described above, the failure of the cathode to anode epoxy seal has prevented us from obtaining long term testing data of the membranes. In the next reporting period, we will study the replacement of the epoxy seals with a glass type seal that have proven successful in the bonding of ceramic to ceramic and ceramic to metal materials in other research programs at Ceramatec.
7. One challenge that needs to be resolved is the absence of undissolved solids in the anolyte solution after the runs. Given the low solubility of sulfur in MF at ambient temperature (< 0.1M), one would expect to find precipitated sulfur in the anolyte. However, this has not been the case, even in the runs where 90%+ sodium recovery was achieved. Atomic sulfur should be the final and most oxidized species in the chain of oxidation reactions that the polysulfide ion species go through. During the next reporting period, we will try to further understand the oxidation reactions occurring in the anode side of the cell in an effort to solve this mystery. Also, a total sulfur content of the anolyte prior to and after the test will be conducted.

Table 7. Sodium recovery test cells assembled and tested during the reporting period

Cell ID#	Anolyte	Anode Electrode	Membrane	Catholyte	Cathode Electrode	Seal Type	Operating Conditions
Na_molten_20101005	0.02 M Na2S4 in TG	Titanium foil (1.0" diam.)	NaSICON GY (0.5 mm thick, 0.8" diam.)	Molten Na	Molten Na, Ti rod current collector	Epoxy Duralco 4461	Temperature=110C No anolyte agitation Cte DC current=1-3 mA
Na_molten_20101015	0.1 M Na2S4 in 15% MF +85% TG	Titanium foil (1.1" diam.)	NaSICON GY (0.72 mm thick, 0.8" diam.)	Molten Na	Molten Na, Ti rod current collector	Epoxy Duralco 4461	Temperature=110C Anolyte agitation Cte DC current=1-3 mA
Na_molten_20101026	0.05 M Na2S4 in 25% MF +75% TG	Titanium foil (1.1" diam.)	NaSICON GY (1 mm thick, 0.8" diam.)	Molten Na	Molten Na, Ti rod current collector	Epoxy Duralco 4461	Temperature=110-115C Anolyte agitation Cte DC voltage=6 V
Na_molten_20101105	0.1 M Na2S4 in 50% TG +50% MF	Titanium foil (1.1" diam.)	NaSICON GY (1 mm thick, 0.8" diam.)	Molten Na	Molten Na, Ti rod current collector	Epoxy Duralco 4461	Temperature=110-115C Anolyte agitation Cte DC voltage=6 V
Na_molten_20101109	0.1 M Na2S4 in MF	Titanium foil (1.1" diam.)	NaSICON GY (1 mm thick, 0.8" diam.)	Molten Na	Molten Na, Ti rod current collector	Epoxy Duralco 4461	Temperature=110-115C Anolyte agitation Cte DC voltage=5-6 V
Na_molten_20101110	0.3 M Na2S4 in MF	Titanium mesh (1.1" diam.)	NaSICON GY (1 mm thick, 0.8" diam.)	Molten Na	Molten Na, Ti rod current collector	Epoxy Duralco 4461	Temperature=110-115C Anolyte agitation Cte DC voltage=5-6 V
Na_molten_20101115	0.345 M Na2S4 in MF	Titanium mesh (1.1" diam.)	NaSICON GY (1 mm thick, 0.8" diam.)	Molten Na	Molten Na, Ti rod current collector	Epoxy Duralco 4461	Temperature=110-115C Anolyte agitation Cte DC voltage=5-6 V
Na_molten_20101116	0.30 M Na2S4 in MF	Titanium mesh (1.1" diam.)	NaSICON GY (1 mm thick, 0.8" diam.)	Molten Na	Molten Na, Ti rod current collector	Epoxy Duralco 4461	Temperature=110-115C Anolyte agitation Cte DC voltage=5 V
Na_molten_20101119	0.5 M Na2S4 in MF	Platinized Ti mesh (1.1" diam.)	NaSICON GY (1 mm thick, 0.8" diam.)	Molten Na	Molten Na, Ti rod current collector	Epoxy Duralco 4461	Temperature=110-115C Anolyte agitation Cte DC voltage=5 V
Na_molten_20101129	0.46M Na2S4 in MF	Platinized Ti mesh (1.1" diam.)	NaSICON GY (1 mm thick, 0.8" diam.)	Molten Na	Molten Na, Ti rod current collector	Epoxy Aremco 631	Temperature=120C Anolyte agitation Cte DC voltage=5 V
Na_molten_20101208	0.254 M Na2S4 in MF	Platinized Ti mesh (1.1" diam.)	NaSICON GY (1 mm thick, 0.8" diam.)	Molten Na	Molten Na, Ti rod current collector	Epoxy Aremco 631	Temperature=120C Anolyte agitation Cte DC voltage=5 V
Na_molten_20101215	0.254 M Na2S4 in MF	Platinized Ti mesh (1.1" diam.)	NaSICON GY (1 mm thick, 0.8" diam.)	Molten Na	Molten Na, Ti rod current collector	Epoxy Aremco 631	Temperature=120C Anolyte agitation Cte DC voltage=5 V

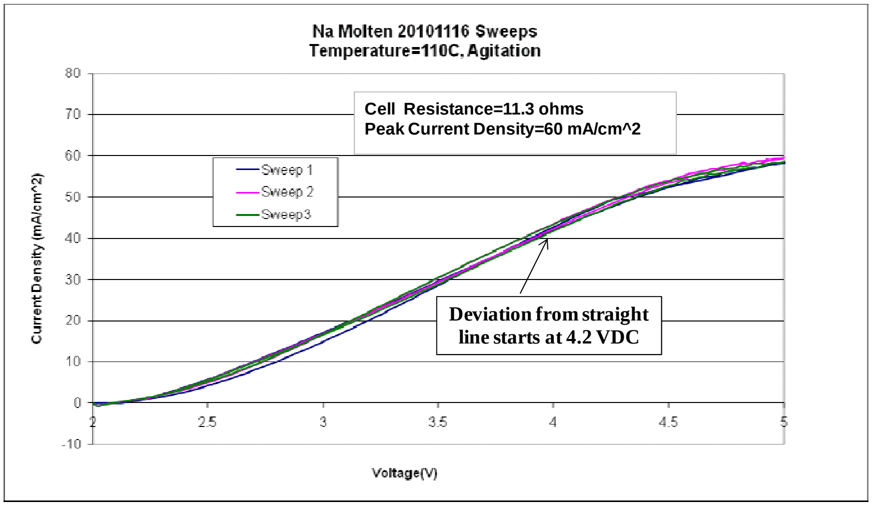

Figure 6. Voltage sweeps between 2 and 5 Volts for molten sodium recovery cell *Na_molten_20101116*

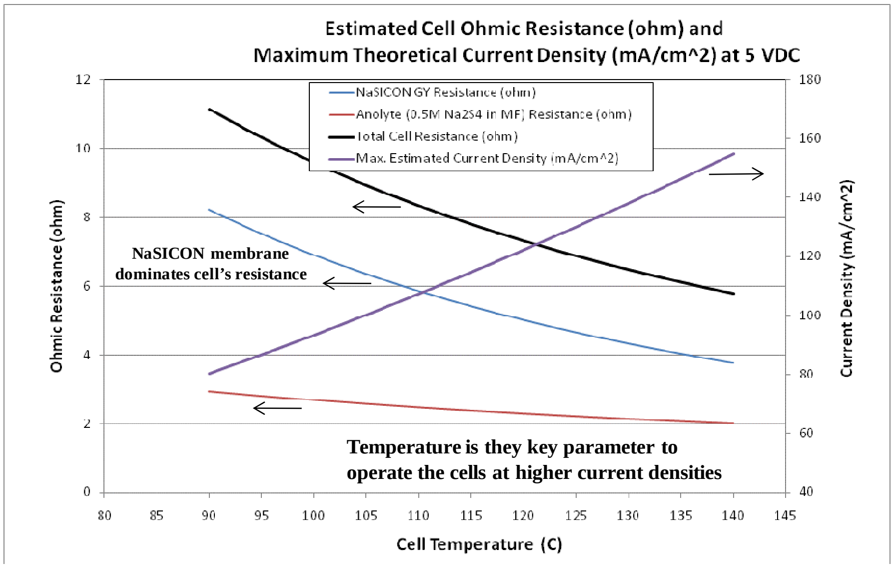

Figure 7. Predicted ohmic resistances of anolyte solution (0.5 M Na_2S_4 in MF) and NaSICON GY membrane (1 mm thick); and maximum cell current density versus cell operating temperature. Model assumes no mass transfer limitation and OCV=2.1VDC. NaSICON-GY ionic conductivity data by *J. Watkins (2008)*

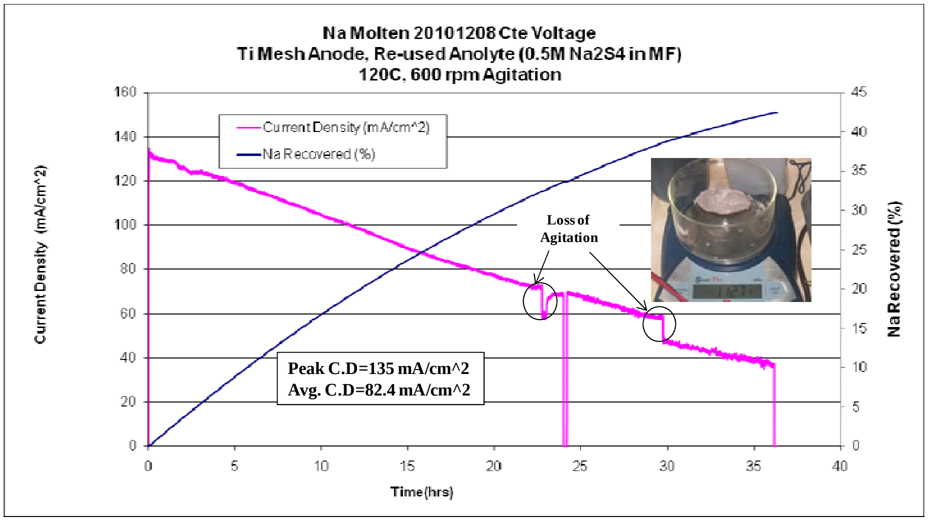

Figure 8. Cell current density and sodium metal recovery percentage versus run elapsed time for sodium recovery cell *Na_molten_20101208*

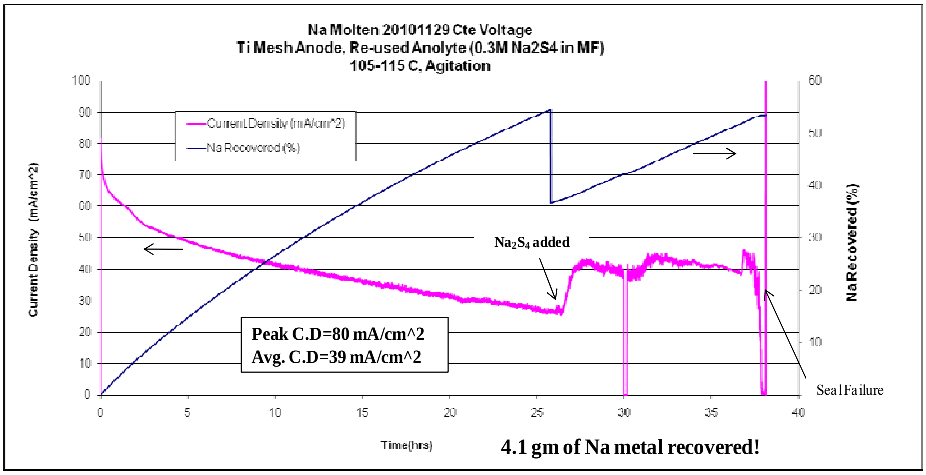

Figure 9. Cell current density and sodium metal recovery percentage versus run elapsed time for sodium recovery cell *Na_molten_20101129*

Lithium Recovery Test Runs

A total of six lithium recovery test runs were conducted in this period. All the tests were done using the new Dual Test Flow Cells in both batch and closed-loop continuous modes. Table 8 summarizes the cell construction properties and the runs operating conditions. The first three runs were conducted in batch mode with the catholyte (LiI in TG) and anolyte (Li_2S in MF) solutions sealed in the cathode and anode compartments, respectively. The first cell was run inside the lab furnace at 50ºC, whereas the other two were run at ambient temperature. In the batch mode, pressurization of the catholyte compartment is expected, due to volume reduction, as the lithium metal is plated on the electrode. Therefore, only limited amount of run time was allowed to avoid bursting of the cells. The purpose of these initial batch runs was to evaluate the overall performance of the cell and to determine whether any design changes would be needed in preparation for the closed-loop continuous runs. Three runs in closed-loop continuous mode were completed in this reporting period, all of them at ambient temperature. Unfortunately, we faced at lot of issues related to materials of construction compatibility of the lab equipment (e.g. o-rings, tubing, etc.). This prevented us from obtaining long term testing data. The main conclusions learnt from these runs are summarized below.

1. Similarly to our previous findings with the glass test cells, Cyclic Voltammetry data (Figure 10) shows that the lithium reduction reaction is very selective within the cell voltage range of interest (2 to 6 VDC). In the particular case plotted here, the current vs. voltage curve remained linear within the voltage range swept, which indicates that no mass transfer limitation was reached during the measurement.
2. A maximum current density of 11 mA/cm^2 was measured at 50ºC, whereas approximately half of that value was obtained when the cells were run at ambient temperature. This is explained by the higher ionic conductivity of both LiSICON membrane and electrolytes at the higher temperature. Unfortunately, the ambient temperature data shows that the cells suffer significant deactivation only after a few hours of operation at constant voltage. Figure 11 shows this for *Li Recovery Dual Flow 20101222* cell. The cell ran at 2.5 mA/cm^2, for approximately 5 hours, and then dropped down to 1 mA/cm^2 over a period of four hours. This current density level was maintained for the remaining of the test. One of the leading hypotheses to explain the cell polarization is the increase of the electronic resistance across the cathode electrode surface due to its coverage with solvent-wetted lithium metal.

Formatted: Bullets and Numbering

3. The data from the batch runs indicate that vertical cell orientation is preferred over the horizontal arrangement as indicated by the lower operating voltage. The vertical orientation assures that any air trapped inside the cell during the electrolyte loading stays up and out of the membrane or electrode surfaces.
4. Varying the electrolytes flow rate had no measurable effect on the cell's operating current density. This indicates that, at ambient temperature, the rate of the redox reactions are not controlled by mass transport of the ionic species across the electrodes or membrane interfaces.
5. Lithium plates as small granular particles that stick to each other and are wetted with catholyte solvent. Figure 12 displays the top and side views of a typical lithium metal deposit on the titanium mesh electrode of a Dual Flow Test Cell. The standard operating procedure

of the tests is to stop the cell, after some time, to remove the lithium deposit. After the electrode surface is wiped clean the run is resumed.

6. The reliability of the 1.5” in diameter LiSICON 10B membranes, used in the Dual Flow Cells, has been outstanding so far. As reported previously, the anode side of the membranes displays an intense blue coloration (Figure 13). We know that this color change starts to occur as soon as power is applied to the cell. The colored layer is very thin and it does not seem to affect the performance of the cell. Unfortunately, we still do not have long term testing data (>30 hours) at higher current densities (>5mA/cm^2) to fully evaluate the membranes. We expect to generate this data during the next quarter.

Table 8. Lithium recovery test cells assembled and tested during the reporting period

Cell ID#	Anolyte	Anode Electrode	Membrane	Catholyte	Cathode Electrode	Operating Conditions
Li_Recovery_Dual Flow_Cell_20101029	0.5 M Li2S in MF	Glassy carbon plate (1.65"x1.75", 1 mm thick) 4 mm to membrane	LiSICON 10B 1.5" Diam., 1 mm thick	1M LiI in TG	Titanium mesh (1.65"x1.75", 0.2 mm thick) 5 mm to membrane	Batch, Temperature=50C Cte Current=30 mA
Li_Recovery_Dual Flow_Cell_20101103	0.5 M Li2S in MF	Glassy carbon plate (1.65"x1.75", 1 mm thick) 4 mm to membrane	LiSICON 10B 1.5" Diam., 0.5 mm thick	1M LiI in TG	Titanium mesh (1.65"x1.75", 0.2 mm thick) 5 mm to membrane	Batch, Temperature=21C Cte Current=30 mA
Li_Recovery_Dual Flow_Cell_20101109	0.3 M Li2S in MF	Glassy carbon plate (1.65"x1.75", 1 mm thick) 1 mm to membrane	LiSICON 10B 1.5" Diam., 0.5 mm thick	1M LiI in TG	Titanium mesh (1.65"x1.75", 0.2 mm thick) 5 mm to membrane	Batch, Temperature=21C Cte Voltage=6V
Li_Recovery_Dual Flow_Cell_20101206	0.3 M Li2S in MF	2 Graphite foils glued together (1.65"x1.75", 1 mm thick) 5 mm to membrane	LiSICON 10B 1.5" Diam., 1 mm thick	1M LiI in TG	Glassy carbon plate (1.65"x1.75", 0.5 mm thick) 2 mm to membrane	Continuos closed loop mode Temperature=21C Cte Voltage=6V
Li_Recovery_Dual Flow_Cell_20101210	0.2 M Li2S in MF	Platinized Ti plate (1.65"x1.75", 0.2 mm thick) 2 mm to membrane	LiSICON 10B 1.5" Diam., 1 mm thick	1M LiI in TG	Titanium mesh (1.65"x1.75", 0.2 mm thick) 5 mm to membrane	Continuos closed loop mode Temperature=21C Cte Voltage=6V
Li_Recovery_Dual_Flow_Cell 20101222	0.2 M Li2S in MF	Glassy carbon plate (1.65"x1.75", 0.5 mm thick) 3 mm to membrane	LiSICON 10B 1.5" Diam., 1 mm thick	1M LiI in TG	Titanium mesh (1.65"x1.75", 0.2 mm thick) 5 mm to membrane	Continuos closed loop mode Temperature=21C Cte Voltage=6V

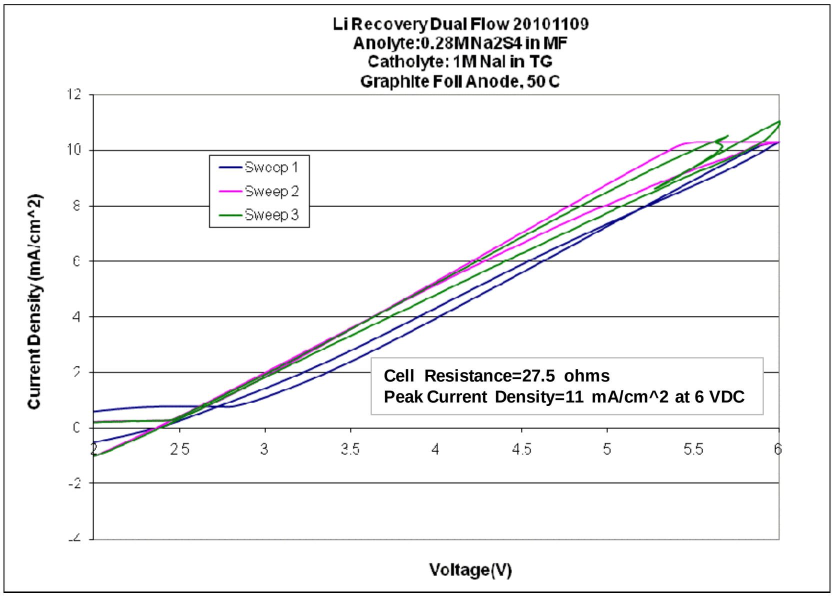

Figure 10. Current density vs. cell voltage (voltage sweep) for *Li Recovery Dual Flow 20101109* cell, run in batch mode at 50ºC

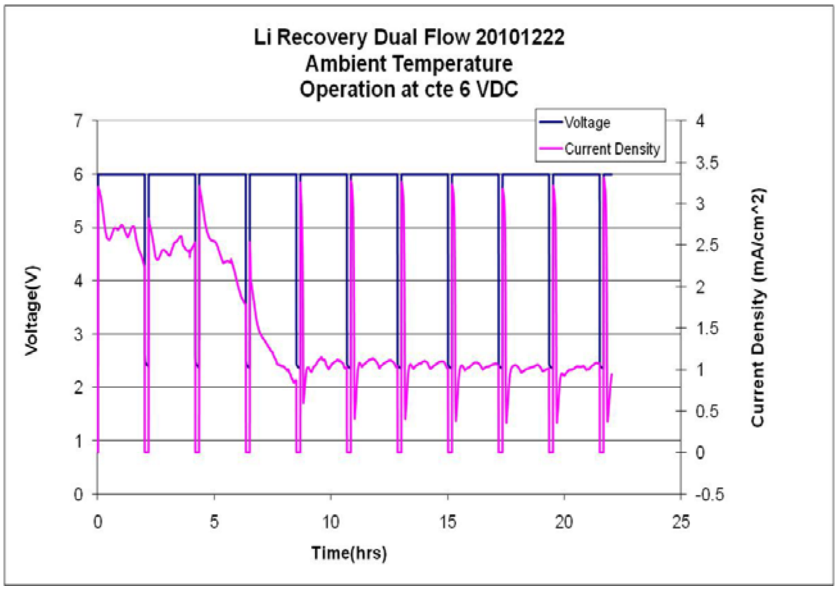

Figure 11. Current density vs. time, at 6 VDC constant voltage, for *Li Recovery Dual Flow 20101222* cell, run in closed loop continuous mode at ambient temperature

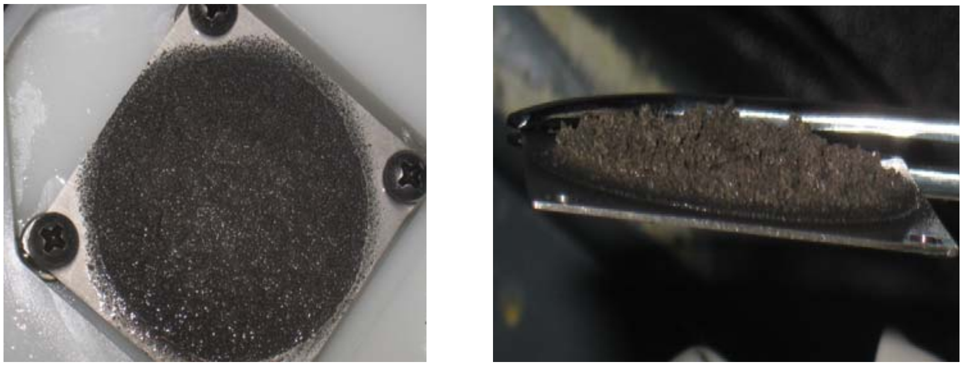

Figure 12. Top [A] and side [B] views of lithium metal deposit on the cathode electrode surface

Figure 13. Anode [A] and Cathode [B] sides of the LiSICON 10B membrane after disassembly from *Li Recovery Dual Flow Cell 20101029*

Task 4.0 – Analysis

Subtask 4.1 – Develop upgrading process model

Ceramatec shall evaluate several process variables in Task 2 which will impact the effectiveness of impurity removal, saturation, coking, and alkali metal utilization. In addition, the shale oil source and initial composition is likely to be a factor. Extent of hydrogen donation gas added and presence of hydrotreating catalyst will affect the extent of upgrading. A preliminary model based on the data from Task 2 will be constructed.

The Recipient shall model the upgrading process constructed in Phase 1. The design model of separation scheme of Task 3 will be added to the overall model of upgrading process.

Methodology

Modeling of the upgrading process is in progress. A basic methodology has been laid out. The modeling exercise constitutes mass and energy balances of the overall process. These calculations will be related to operating costs as we proceed further. Listed below are the results of modeling exercise to-date. Figure 14 shows the key components required for the process. The reactor is filled with the crude oil sample. Sodium and compressed hydrogen/methane are pumped into the reactor separately. Oil reacts with Na, H_2/CH_4, and partial amount of H_2S to form sodium sulfide and sodium nitride. Sodium nitride further reacts with H_2S to form sodium sulfide and ammonia gas is released. In a separator, sodium sulfide and heavy metals are separated from the upgraded oil. Sodium sulfide, so formed, is sent to the electrolytic cell for recovering sodium and sulfur. Recovered sodium is again recycled into the reactor.

Formatted: Font: Not Bold

Deleted: Figure

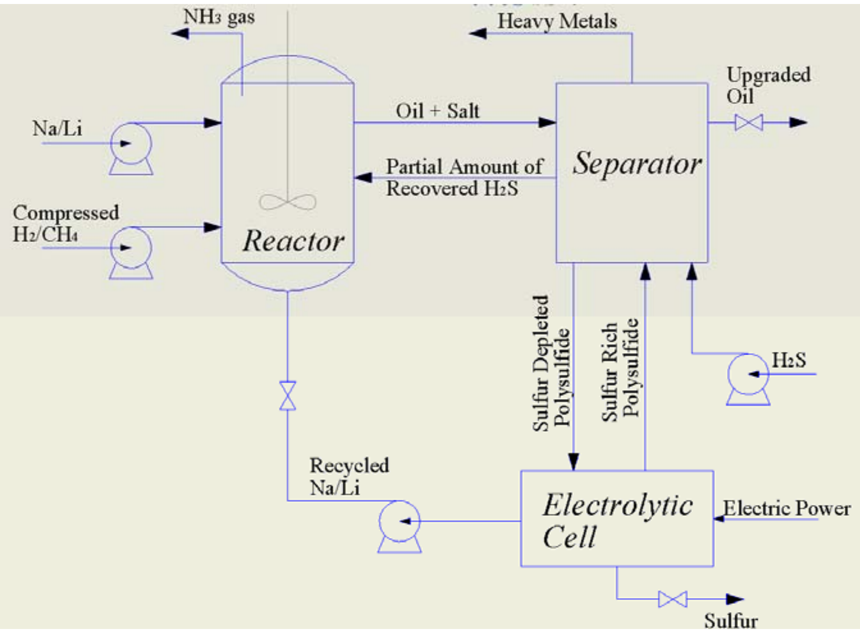

Figure 14: Flow diagram of oil processing showing key components

Analytical approach to calculate the mass and energy consumption in the reactor is followed. It has been assumed (for the sake of simplicity) that sulfur and nitrogen are present in oil in the form of hetero atom bearing compounds such as Thiophene and Pyridine. When Na is used as a desulfurization and denitrogenation agent, there are four possible reactions in the reactor as listed in Table 9. The structure of the chemical compounds appeared in Table 9 is shown in Table 10.

Table 9: Primary reactions occurring in the reactor

Reactions		Reactants	Products
Sulfur removal	1	Thiophene + 2Na + H_2 =	Na_2S + Butadiene
	2	Thiophene + 2Na + CH_4 =	Na_2S + Pentadiene
Nitrogen removal	3	Pyridene + 3Na + $1.5H_2$ =	Na_3N + Pentadiene
	4	Pyridene + 3Na + $1.5CH_4$ =	Na_3N + 0.5Hexadiene + 0.5Heptadiene

Table 10: Details of the primary compounds used in the reactor

Compound Name	Structure	Mass (g/mole)
Thiophene C_4H_4S	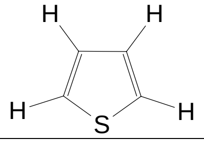	84.1356
Pyridine C_5H_5N	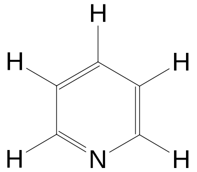	79.1012
1,3-Butadiene C_4H_6	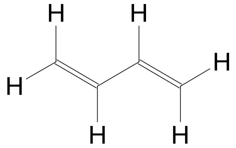	54.0914
1,3-Pentadiene C_5H_8	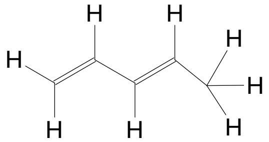	68.1182
1,4-Hexadiene C_6H_{10}	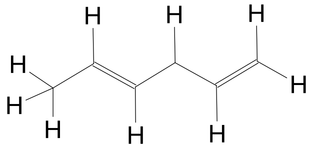	82.145
1,6-Heptadiene C_7H_{12}	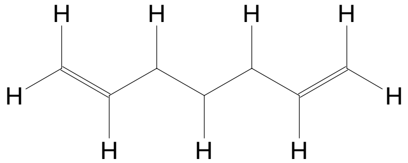	96.1718

Mass balance of the reactor

In the mass balance model, two processes are defined. Process 1 involves treating with H_2 and process 2 involves treating with CH_4. Table 11 shows the raw data of oil samples.

Table 11: Raw data of the oil samples

Feed	RL	OSEC	SJ
C (%)	84.48	84.83	85.7
H(%)	12.33	12.74	11.27
S(%)	0.25	0.84	1.54
N(%)	1.48	0.47	0.76
API gravity	35.29	35.29	10.78
Density (g/cc)	0.848	0.848	0.995

Following is the step by step approach used to calculate H/C ratio.

a. First the balanced reactions as shown in Table were noted down.
b. Mass of the reactants in reaction 1 (Thiophene, Na, and H_2), equivalent to the mass of sulfur per 100 g of oil sample, were calculated.
c. Mass of the products in reaction 1 (Butadine and Na_2S), equivalent to the mass of sulfur per 100 g of oil sample, were calculated.
d. Steps b and c were followed for reaction 3 to find the equivalent mass of reactants and products for the mass of nitrogen per 100 g of oil.
e. Mass of the remaining portion of oil is calculated by subtracting 'b + d' from 100 g.
f. Mass of C & H present in the reactant part of the reactions 1 and 3 was calculated.
g. Ratio H/C of reactants i.e. $(H/C)_{in}$ was calculated.
h. Mass of C & H present in the product part of the reactions 1 and 3 was calculated.
i. Ratio H/C of products i.e. $(H/C)_{out}$ was calculated.
j. %Δ(H/C) was calculated. Higher the value of %Δ(H/C), more is the energy gained in the process.
k. Exactly same procedure is followed for process 2.

Deleted: Table

Formatted: Bullets and Numbering

Table 12 shows the results of %Δ(H/C) for the known oil samples. Heat of combustion associated with $(H/C)_{out}$ can be calculated from Figure 15 below. A linear curve was fitted through the data points. This plot helps to interpolate for intermediate values and gives accurate value of heat of combustion for the corresponding value of H/C.

Deleted: Table

Deleted: Figure

Table 12: %Δ(H/C) ratio for the oil samples

Feed	Process 1 (H2)	Process 2 (CH4)
RL	3.5087	3.002
OSEC	2.001	1.324
SJ	3.105	2.766

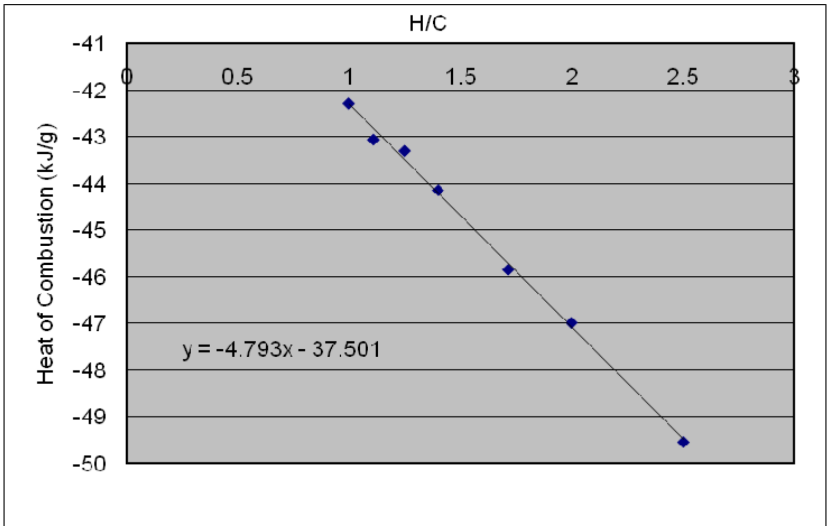

Figure 15: Heat of combustion (kJ/g) versus H/C

Energy balance of the reactor

The basic energy model of the reactor is shown in Figure 16. Reactants enter the reactor and reaction is carried out at 375 C (707 F). By the law of conservation of energy principle,

$$\begin{bmatrix} \text{Total energy transfer} \\ \text{by heat, work, and mass} \end{bmatrix} = \begin{bmatrix} \text{Change in internal,} \\ \text{kinetic, and potential energies} \end{bmatrix} \ldots\ldots\ldots\ldots\ldots\ldots\ldots (1)$$

$$[dQ + dW + dEm] = [dU + d(KE) + d(PE)] \ldots\ldots\ldots\ldots\ldots\ldots\ldots\ldots\ldots\ldots\ldots\ldots\ldots\ldots (2)$$

where,

dQ is the net heat transfer for the reactor = $Q_{in} - Q_{out}$
dW is the net work transfer for the reactor = $W_{in} – W_{out}$
dEm is the energy transfer due to the net mass transfer for the reactor = $Em_{in} - Em_{out}$
dU is the change in the internal energy of the reactor
d(KE) and d(PE) are the change in kinetic and potential energy of the reactor

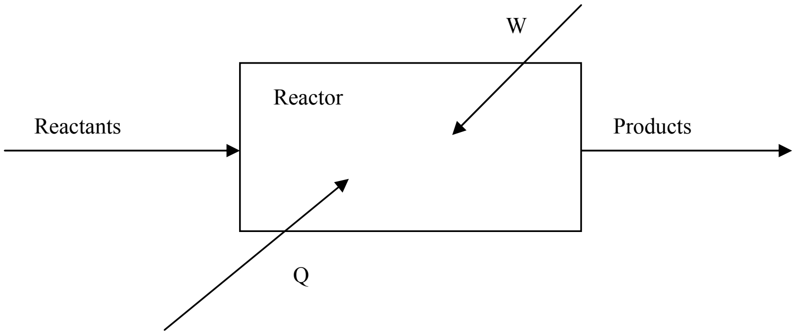

Figure 16: Conceptual reactor model for energy balance

In an experimental set up the reactor, initially, is filled with oil sample and an alkali metal. The reaction is carried out for 1 to 2 hours in the reactor. During this time reactor is closed and no mass is flowing in and out of the system. For a closed system, dEm, d(KE), and d(PE) are zero. Products forming in the reactor are sent to the separator. Input configurations of the separator are not known yet and hence, Q_{out} is neglected in this preliminary report. The reactor is not performing any mechanical work and so, W_{out} does not exist. Change in internal energy can be expressed as,

$$dU = dH - PdV \quad \ldots\ldots\ldots\ldots\ldots\ldots\ldots(3)$$

For a liquid oil sample, there is no appreciable change in volume and so change in internal energy is merely a change in an enthalpy value. For chemical reactions, total enthalpy change is expressed as,

$$dH = d(h_T - h_0) \pm dH_{rxn} \quad \ldots\ldots\ldots\ldots\ldots\ldots (4)$$

The term in the parentheses represents the sensible enthalpy relative to the standard reference state, which is the difference between h_T (the sensible enthalpy at specified state of 375 C) and h_0 (the sensible enthalpy at standard referenced state of room temperature). At the preliminary stage, it is assumed that there is no appreciable change in the sensible heat of the reactants and product, and therefore, $d(h_T - h_0)$ is assumed to be zero. The second term dH_{rxn}, the enthalpy of reaction, is the energy generated or absorbed as a result of chemical reaction. Enthalpy of reaction is the subtraction of enthalpy of formation of reactants from the enthalpy of formation of products. dH_{rxn} is positive or negative depending on the type of reaction i.e. exothermic or endothermic. From equations (2) to (4) and with the stated assumptions, total energy consumption for the reactor part is,

$$E = Q_{in} + W_{in} \pm dH_{rxn} \ldots\ldots\ldots\ldots\ldots\ldots (5)$$

Q_{in} is the energy required to heat the reactor to 375 C, which is $m*C_p*dT$. All the calculations carried out in this report are based on per 100 g of oil and so, m is 0.1 kg. C_p, the specific heat, is the specific heat of shale oil, which is 2.0934 kJ/kg-K. The temperature difference dT is 350 C, assuming room temperature of 25 C. Calculated value of Q_{in} is 72.85 kJ. Work is done on the system and so, it contributes towards the energy consumption. It is assumed negligible compared to heat input for raising the temperature of the reactor.

Lastly, the energy generated as enthalpy of reaction is calculated for reactions mentioned in Table 13. Enthalpies of reactions, so calculated, are in the form of J/mole. Energy is calculated by multiplying the enthalpy of reaction by the number of moles of Thiophene and Pyridine per 100 g of oil sample. Table 13 lists the enthalpies of reactions for the reactions listed in Table 9.

Deleted: Table

Table 13: dH_{rxn} for reactions shown in Table 9

Reaction type	Reaction #	dH_{rxn} (kJ)
Sulfur removal Reactions	1	-2.920
	2	-2.45
Nitrogen removal reactions	3	-120.170
	4	-101.916

Subtask 4.2 – Develop electrolysis process model

Ceramatec shall analyze data from Task 3 and a performance model will be developed. Various factors such as membrane thickness, type of alkali metal, electrode configuration and cell design would be included in the model considerations.

The overall electrolysis process is sketched in Figure 17 with all the input and output streams. A low sulfur to alkali metal ratio polysulfide (M_2S_x) solution stream and a make-up fresh solvent stream enter the process. Three output streams consisting of a high sulfur to alkali metal polysulfide (M_2S_y) solution, sulfur, and alkali metal (M) leave the process. In the figure M could be sodium or lithium and the index y is greater than x. Electrical power to drive the electrolysis reactions, pump the electrolytes, maintain the cell operating temperature, and others is needed.

Since the single largest operating cost of the process is the electric power required for the electrolysis reactions to occur, minimizing the cell voltage should be one main optimization goals. The specifics of the electrolysis process are highly dependent on the alkali metal that needs to be recovered. Figures 18 and 19 show the schematics of two proposed processes to recover sodium and lithium metal, respectively. The anolyte side of the two processes is basically identical. The polysulfide salts (M_2S_x) are transported into the anolyte mixing tank, where they are dissolved into the anolyte solvent and heated up to the cell operating temperature. A recycled stream of the polysulfide (M_2S_y) solution can be returned back to the cell for further sulfur and alkali metal recovery. The low solubility of sulfur in the anolyte solvent will make it to precipitate as it forms in the cell. Therefore, the output stream of the cell will consists of a slurry containing the undissolved sulfur and the dissolved polysulfides. The stream is first cooled and then transported into a sedimentation tank, where the light and the slurry phases are separated. The slurry phase is then washed and the solid sulfur filtered in a rotary vacuum-drum filter. The polysulfide solution is then pumped into the anolyte storage tank. From the tank, a main stream is returned to the oil upgrade reaction/separation process and a smaller stream is recycled back to the anolyte mixing tank. So, where the lithium and sodium processes differ is on the catholyte side. While molten sodium is the catholyte in the sodium recovery process, a non-molten organic solvent catholyte is used for lithium recovery. Molten sodium is continuously removed from the cathode chamber at the same rate at which it is being produced. The molten metal is pumped to molten sodium storage tank from where is transported to the oil upgrade reactor. During the startup operations, the cell will be primed with molten sodium from the storage tank. A recycled stream can be returned to the cell during continuous operation to further enhance mixing within the cathode compartment. Due to the high melting temperature of lithium, an organic solvent based catholyte, with a dissolved supporting electrolyte, is preferred for the separation of lithium. Lithium metal is plated at the cathode electrode, from where it can be removed in continuous or batch operating mode. The catholyte solution is continuously circulated through the cell from a mixing tank, where make-up catholyte solvent can be added as needed. It is advantageous to the process to maintain a high flow rate through the cell to achieve good mixing through the electrode and ceramic membrane interfaces.

Table 14 lists the expected range of operating conditions and properties of construction of the cells. Narrowing down the final cell operating conditions will be accomplished through process and cost optimization and further experimental data analysis. Table 15 displays the importance of operating current density and the overall cell voltage on power consumption (operating cost) and total cell area needed (capital cost).

Over the next reporting period, detail mass and energy balances of the two proposed processes will be conducted.

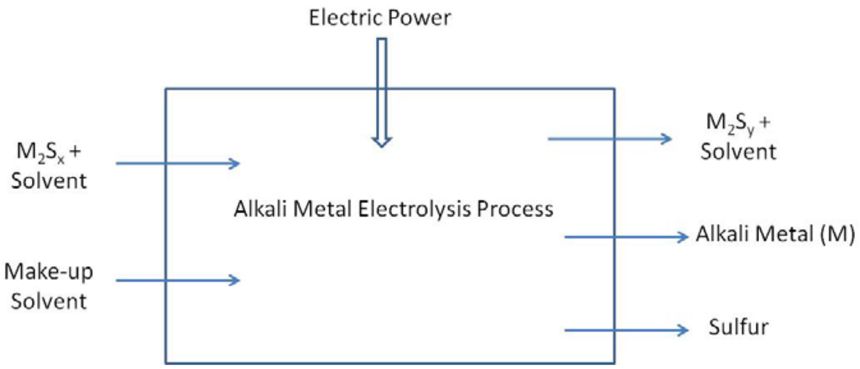

Figure 17. Simplified alkali metal electrolytic recovery process schematic.

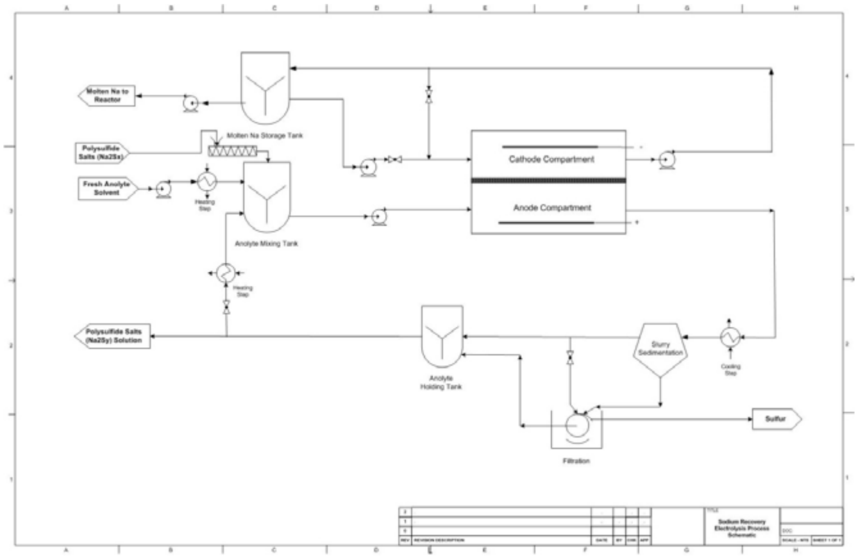

Figure 18. Schematic of the sodium electrolytic recovery process

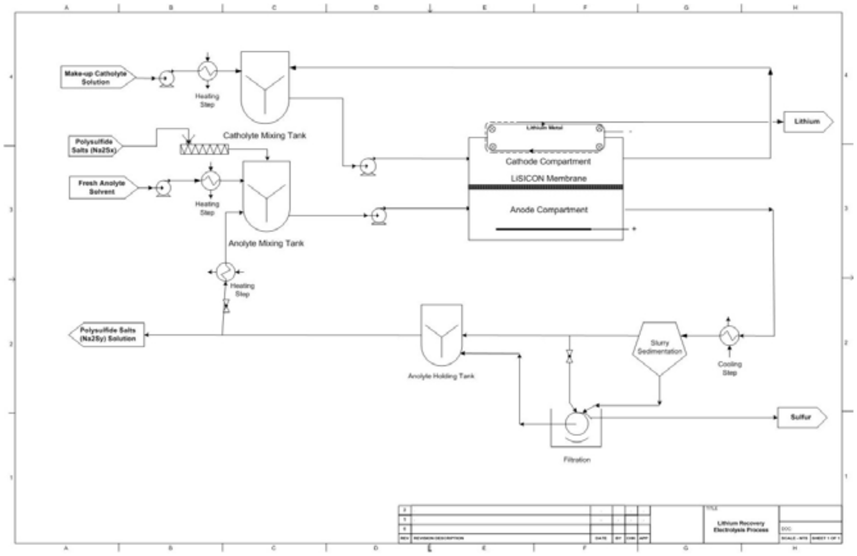

Figure 19. Schematic of the lithium electrolytic recovery process

Table 14 Operating conditions of sodium and lithium recovery cells

Cell Type	Temperature	Current Density Target	Maximum Voltage	Catholyte	Anolyte	Membrane Type	Membrane Thickness
	C	mA/cm^2	V				microns
Sodium	120-160	100 to 200	5	Molten Na	Polysulfides in MF	NaSICON GY	500 to 1000
Lithium	120-160	100 to 200	6	NaI in TG	Polysulfides in MF	LiSICON 10B	500 to 1000

Table 15 Estimated power consumption (electrolysis only) and specific area requirements for sodium and lithium recovery cells

Cell Type	Current Density	Maximum Cell Voltage	Power Consumption for Electrolysis only		Specific Cell Area Requirements	
			For S	For N	For S	For N
	mA/cm^2	V	Kw-h/Kg S	Kw-h/Kg N	m^2-h/kg S	m^2-h/kg N
Sodium	100	5	8.36	28.72	1.67	5.74
Sodium	200	5	8.36	28.72	0.83	2.87
Lithium	100	6	10.03	34.46	1.67	5.74
Lithium	200	6	10.03	34.46	0.83	2.87

.

Subtask 4.3 – Preliminary cost analysis

The Recipient shall incorporate the models from Subtasks 4.1 and 4.2 into a preliminary cost model. Based on the preliminary cost analysis, a selection will be made between sodium and lithium as the most promising alkali metal for further pursuit in Phase 2.

No progress on this task to date.

Task 5.0 – Reporting

The 5th Quarterly Report is presently submitted.

CONCLUSION

Our conclusion at this point is that levels of both sulfur and nitrogen can be removed from shale oil with the process tested. More optimization is required. So far the process has been effective with shale oil and with Heavy Oil. Sodium results appear to be more effective than lithium in the upgrading process.

COST STATUS

The monthly costs of the 5th quarter are shown in Table 16, along with the projected costs stated in the Project Management Plan.

Table 16. Project costing profile for the 5th Quarter

		Oct-10		Nov-10		Dec-10		Q5	
		Projected	Actual	Projected	Actual	Projected	Actual	Projected	Actual
Direct Labor			30,596.78		24,850.79		19,832.73		75,280.30
Benefits	32%		9,790.97		7,952.25		6,346.47		24,089.69
Overhead	41%		12,544.68		10,188.82		8,131.42		30,864.92
Total Burdened Labor			52,932.43		42,991.86		34,310.62		130,234.91
Direct Materials / Spec Test			26,941.25		29,258.96		25,704.06		81,904.27
Equipment			23,490.00						23,490.00
Travel			1,067.68				-		1,067.68
Subtotal			104,431.36		72,250.82		60,014.68		236,696.86
G&A	29%		30,285.09		20,952.74		17,404.26		68,642.09
Total monthly		-	134,716.45	-	93,203.56	-	77,418.94	-	305,338.95

Our costs in the 5th quarter were moderately than the projection because there was a lag in ordering equipment early in the project that carried through. Overall the project is behind in spending by approximately 2% over the first 15 months.

Figure 20 shows a plot of the total monthly costs and the initially projected costs versus time and Figure 21 shows the cumulative monthly costs versus time. Also shown in Figure 21 is the fraction of actual over planned cumulative expenses.

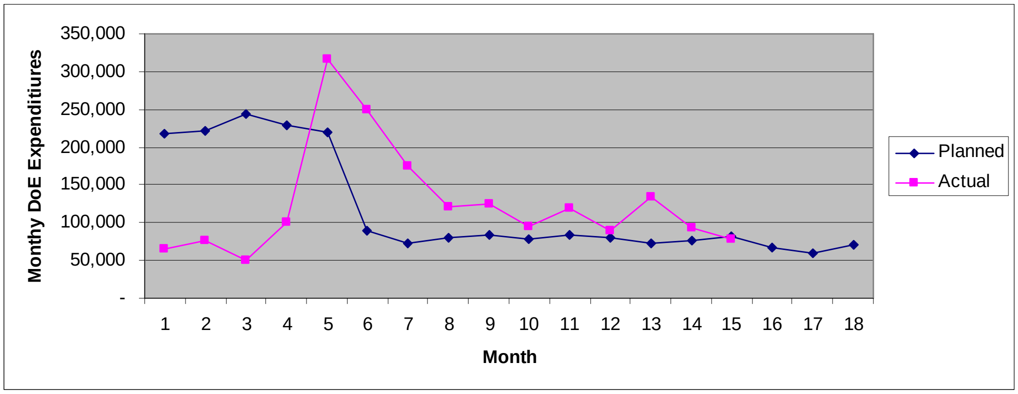

Figure 20: Projected and actual monthly costs over time

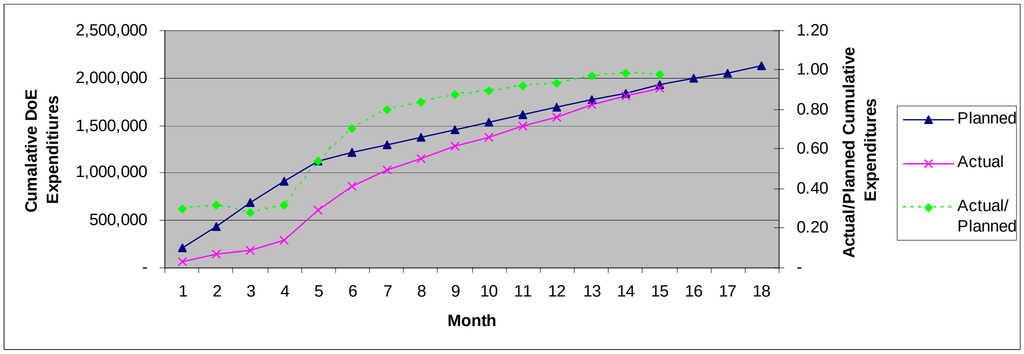

Figure 21: Projected and actual cumulative costs over time

MILESTONE STATUS

Table 17: Milestone log for 3rd Quarter

Milestone No.	Task / Sub-task	Project Milestone Description	Planned Start Date:	Planned End Date:	Actual Start Date:	Actual End Date:	Comments
1	1	Updated PMP	9/29/09	10/29/09	9/29/09	10/26/09	
2	2.1	Analytic capability established	9/29/09	3/1/10	9/29/09	3/23/10	Analytical capability has been established as stated in the PMP. Operators have been trained on GC. ICP and CHNS are operational
3	2.2	Complete upgrading exp. Setup	9/29/09	3/29/09	9/29/09	3/26/10	Upgrading set-up has been completed including HAZOP and pre-start up safety review. The reactor set up has been ready to be operational as of Friday, March 26, 2010.
4	2.3	Complete process runs	3/30/10	1/3/11	3/26/10		Process runs underway
5	3.1.1	Complete membranes for Phase 1	9/29/09	7/5/10	9/29/09	9/20/10	Membrane fabrication has exceeded demand for fabrication. Mechanical characterization was complete on September 20, 2010.
6	3.3	Cells ready for operation	4/13/10	2/28/11	4/13/10		Cells were ready for operation on time. Initial cells testing began running 4/26/10 when sufficient sodium polysulfide was synthesized.
7	4.3	Preliminary cost model complete	2/8/11	3/14/11			

ACCOMPLISHMENTS

- ✓ Electrolysis of sodium sulfide at temperatures of molten sodium have begun and are showing very encouraging results.
- ✓ Reactor tests with methane have continued with encouraging results
- ✓ Process models of both the reactor and electrolysis processes have begun which will lead to the preliminary cost model.

PROBLEMS OR DELAYS

Our Perkin Elmer CHNS analyzer has been unsatisfactory. We have ordered a LECO analyzer as a replacement. In the meantime samples have been sent to an outside lab for analysis.

PRODUCTS

No products to report at this time.

National Energy Technology Laboratory

626 Cochrans Mill Road
P.O. Box 10940
Pittsburgh, PA 15236-0940

3610 Collins Ferry Road
P.O. Box 880
Morgantown, WV 26507-0880

13131 Dairy Ashford, Suite 225
Sugar Land, TX 77478

1450 Queen Avenue SW
Albany, OR 97321-2198

2175 University Ave. South
Suite 201
Fairbanks, AK 99709

Visit the NETL website at:
www.netl.doe.gov

Customer Service:
1-800-553-7681

DEPARTMENT OF ENERGY • UNITED STATES OF AMERICA